ELSEVIER

Catalysis Today 67 (2001) 357–368

CATALYSIS TODAY

www.elsevier.com/locate/cattod

Chemically sensitive parallel analysis of combinatorial catalyst libraries

Christopher M. Snively, Gudbjorg Oskarsdottir, Jochen Lauterbach*

School of Chemical Engineering, Purdue University, West Lafayette, IN 47907-1283, USA

Abstract

This study demonstrates how Fourier transform infrared imaging (FTIR) can be employed as a powerful spectroscopic tool for the parallel investigation of multiple member heterogeneous catalyst systems. FTIR imaging combines the chemical specificity and high sensitivity of infrared spectroscopy with the ability to rapidly analyze multiple samples simultaneously. A new implementation, using a rapid-scan FTIR spectrometer instead of a step-scan FTIR spectrometer, allows much improved data collection times without sacrificing data quality. Using CO adsorption and CO oxidation as model systems, it was established that FTIR imaging is very well suited to high-throughput parallel analysis of adsorbates and reaction products from supported catalyst libraries.

Keywords: Spectral imaging; FTIR spectroscopy; High-throughput screening; Combinatorial catalysis; CO oxidation

1. Introduction

The ultimate goal of the combinatorial approach is to find the optimum formulation, be it pharmaceutical, engineering material, or catalyst, with the minimum amount of research effort. Practically, this is accomplished by a systematic and efficient exploration of the parameter space that controls the properties of the final product. The two key parts to a successful combinatorial approach are the controlled synthesis of a collection of materials with systematic variations in structure and the subsequent high-throughput analysis of libraries of these materials. Speed, through parallel synthesis and characterization, therefore becomes critical for the success of the combinatorial discovery process. The combinatorial approach has great potential in any discipline to optimize systems that have large parameter spaces. Until recently, the combinatorial approach has been utilized mainly by the drug industry, where it has proven very successful in accelerating the process of drug discovery [1–3]. In the past few years, this concept has also been exploited in the field of material science [4]. The present study reports a novel high-throughput screening technique based on FTIR (Fourier transform infrared) spectral imaging for truly parallel screening of libraries of heterogeneous supported catalysts.

1.1. Synthesis and screening of combinatorial materials libraries — an overview

The essence of combinatorial synthesis is the ability to generate large numbers of chemical compositions very quickly. In solid-state chemical synthesis, several methods of rapidly creating variations in chemical composition have emerged. A binary masking scheme was used by Schultz and co-workers [5] to create small arrays of high-temperature

* Corresponding author. Tel.: +1-765-494-4076; fax: +1-765-494-0805.
E-mail address: jochen@ecn.purdue.edu (J. Lauterbach).

0920-5861/01/$ – see front matter
PII: S0920-5861(01)00328-5

superconducting and giant-magneto-resistive thin film materials by sputtering. This idea demonstrates the potential for much higher diversity in sample composition than previous work and has been extended to include several novel deposition technologies. Physical vapor deposition, electron-beam evaporation, radio frequency sputtering, and pulsed-laser ablation can be used as the molecular sources with moving or stationary masks to achieve spatial variations in composition. All these techniques are suited to create catalyst libraries for initial screening. However, they cannot produce very realistic supported catalyst samples, because this approach ignores many important issues, such as reliable manufacturing processes of supported catalysts with promising material compositions, particle size issues, metal–support interactions, and transport limitations. Solution-dispensing methods, developed for the pharmaceutical industry, have recently been extended to inorganic and organometallic catalyst systems. Solutions containing different amounts of several different metal precursor solutions were dispensed onto the supports using automated liquid-dispensing systems [6–10]. In this manner, samples with a variety of compositions of each component can be quickly and reliably synthesized.

When research in traditional combinatorial methods first began, the methods used to screen the combinatorial libraries were the traditional "one sample at a time" techniques. These included FTIR spectroscopy [11], NMR (nuclear magnetic resonance) [12], MS (mass spectrometry) [13], and HPLC (high-performance liquid chromatography) [11,12]. Several novel methods have been recently published for screening catalyst libraries. The first collection of techniques comprises methods based on conventional serial techniques, which have been modified using various automation approaches in order to decrease the screening time. Amongst these are scanning mass spectrometry and REMPI (resonance-enhanced multiphoton ionization) [14–17]. High-throughput scanning mass spectrometry is based on rapidly analyzing the gases from one sample in a combinatorial library at a time in a sequential manner. There are two different approaches to this technique. The first approach uses a single probe composed of coaxial gas delivery and gas analysis tubes. Libraries are analyzed by sequentially placing the tube over each element of the library [18]. This approach is mainly useful for initial screening of deposited libraries due to its gas delivery design. The second approach uses array of microreactors with supported catalysts, coupled with capillary microprobe sampling. Reactants, products, and carrier gas are withdrawn from each microreactor channel using a capillary sampling probe. By repeating this approach for each microreactor, the entire library can be screened [19]. Another high-throughput screening approach is based on photoionization of reaction products using tunable UV lasers [7,8]. Under REMPI conditions, the resulting photoions are detected by an array of microelectrodes in close proximity to the sample. A tunable UV laser beam is passed above the catalysts and microelectrodes placed above the sites then collect the signal. One disadvantage of this technique, however, is that a suitable laser frequency for each species of interest must be known and accessible with the particular experimental setup [7,8].

Truly parallel screening techniques gather data simultaneously from all the elements in a library. This category includes infrared thermography and FTIR imaging. Thermography detects the infrared radiation emitted by objects and has been used to detect activity for exothermic reactions in combinatorial libraries in a truly parallel fashion [20]. However, thermal imaging does not possess the ability to chemically resolve the product composition, which is a key issue when studying catalysts. Here lies the true advantage of FTIR imaging — the ability to gather chemically sensitive information from each library member simultaneously.

2. Experimental setup

2.1. Imaging spectrometer setup

Spectral imaging in the infrared region was first developed for remote sensing, specifically for military and astronomical applications. More recently, spectroscopists in laboratory and industrial settings have adopted spectral imaging. The original approach to the image collection of spatially resolved infrared information was to use a microscope coupled to a dispersive infrared spectrometer [21,22]. The next step was to join a FTIR spectrometer with an IR microscope [23]. These techniques are both mapping approaches. In order to sample radiation from a well-defined region of the sample, a physical aperture is placed in the

beam path. To collect information from an entire sample, this aperture is moved in discrete steps over the selected sampling area. The main drawbacks of this approach are long collection times and limited spatial resolution.

The most recent instrumental advance in FTIR imaging has been the incorporation of focal plane array (FPA) detectors [24,25]. An FPA consists of a large number of very small infrared detectors arranged in a rectangular grid pattern. When incorporated into an imaging system, radiation from different areas of the sample falls on different areas of the detector, allowing both spatial and spectral information to be collected simultaneously. The FPA and the FTIR spectrometer are connected such that the modulation of the IR source by the interferometer is synchronized with the collection by the FPA. In operation, a series of images is collected as a function of interferometer optical path difference. After fast Fourier transformation of the modulated signal, IR spectra are obtained for every spatial location in the image plane. The data can therefore be thought of as a three-dimensional block that spans one spectral and two spatial dimensions (see Fig. 1). The spectral resolution is determined by the optical retardation of the interferometer, and the spatial resolution depends on the optical configuration and wavelength.

FTIR imaging has been applied to the study of biological systems including brain tissue [26], silicone gel in human breast tissue [27], amino acids [28], canine and [29] human [30] bone tissue, and corn tissue [31]. Applications in the non-biological areas have included pre- and post-cure rubber heterogeneities [32], solvent diffusion [33] in a polymer film, semi-crystalline polymers [34], and polymer dissolution by mixed solvents [35]. Diffusion processes in polymer-liquid crystal systems [36] and polymer-liquid crystal composites have also been examined [37]. All these previous studies imaged a single sample. In this study, FTIR imaging is applied for the first time to high-throughput screening of combinatorial libraries, i.e. to examine multiple samples simultaneously.

In all previous studies, FTIR imaging instrumentation consisted of a step-scan FTIR spectrometer as a

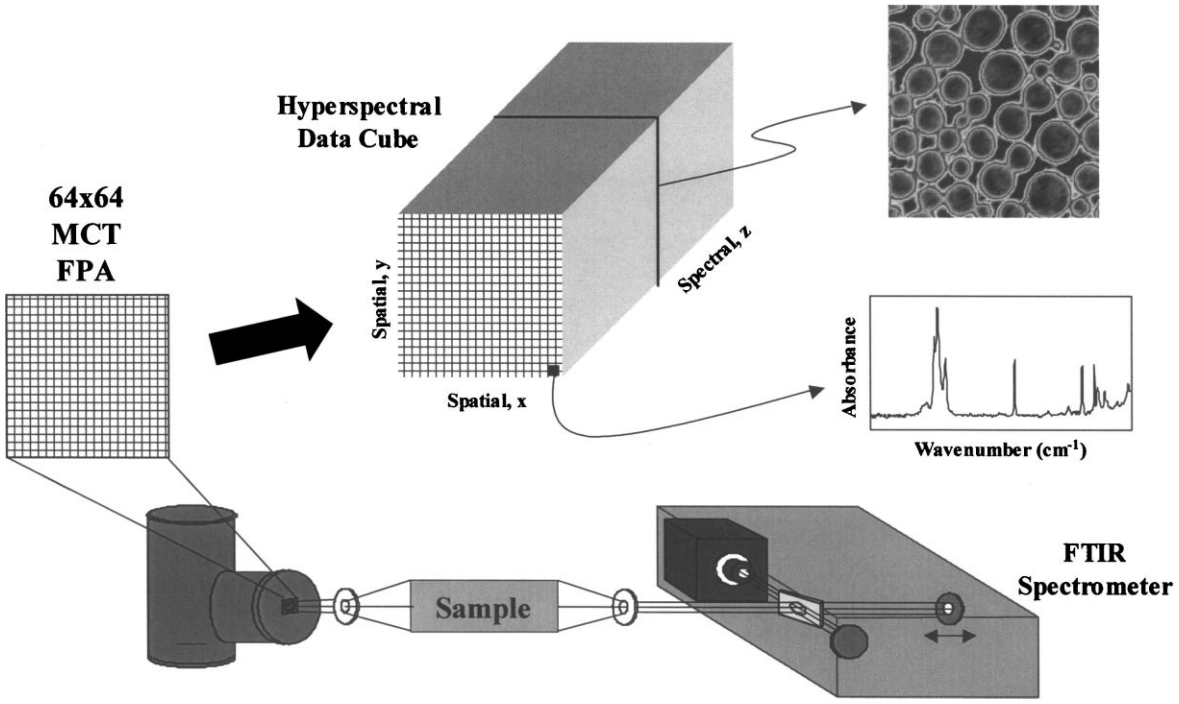

Fig. 1. Basic overview of the FTIR imaging technique.

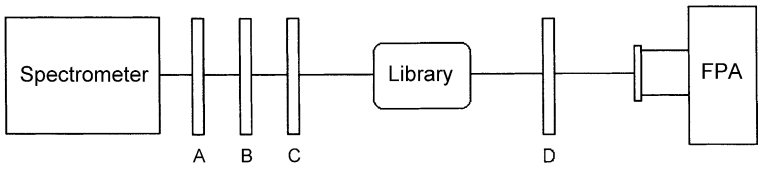

Fig. 2. Block diagram of the imaging setup, showing the layout of the optical components, (A) bandpass filter, (B) diffuser, (C) condensing lens, (D) objective lens.

light source, a microscope with Cassegrainian optics, and FPA detector. To collect a data set, one translates the moving mirror of the interferometer. At specified intervals of mirror travel, the mirror is stopped, and the light intensity values at all pixels are measured. In these previous studies, it had been necessary to collect several frames at each interferogram data point and average these data to obtain a reasonable signal-to-noise ratio (SNR). This collection process, which takes the order of 100 ms per data point, requires that the retardation of the interferometer remain constant during data collection. Therefore, a step-scan spectrometer had to be employed, and the overall collection time of a single data set is 3–15 min on average, depending on the desired spectral resolution and mirror velocity.

Instrumental changes allow us to successfully employ a rapid-scan spectrometer for spectral imaging in the mid-IR [38]. The electronics are sensitive enough to allow the collection of data with a reasonable SNR by acquisition of only one frame per interferogram data point. Since we are acquiring only a single frame at each data point, any artifacts that would result from collecting data over a range of retardation are minimized. In our system, a frame rate of 180 Hz and an integration time (the time span over which light is actually collected) of 180 μs are used. With the moving mirror velocity set at 0.0158 cm s^{-1}, data are collected over a retardation of only 28 nm at each data point, which compares reasonably with the positional accuracy of a step-scan spectrometer. Owing to the decreased collection time of this technique, it becomes practical to average data from several experiments together to increase the SNR, which is common practice in FTIR spectroscopy, without a significant loss of temporal resolution. This averaging technique has been shown to be superior to the technique of collecting multiple frames at each retardation [39]. Overall, the use of a rapid-scan spectrometer has the advantage of reducing the data-collection time by at least an order of magnitude.

A diagram of the optical setup for screening of adsorbates on heterogeneous catalysts is shown in Fig. 2. The setup consists of a Nicolet Magna 860 FTIR spectrometer, calcium fluoride (CaF_2) condensing and refocusing optics, a wide bandpass filter, a KBr diffuser, and a 64×64 pixel mercury cadmium telluride (MCT) FPA detector with dewar and electronics. The bandpass filter is typically employed to minimize Fourier fold-over noise [40].

2.2. Reactor design

The ultimate goal of our research is to study libraries of heterogeneous catalysts by combining the information obtained from parallel reaction product measurements with simultaneous parallel measurements of adsorbates on the catalyst surface. With this approach, we can then systematically correlate fundamental reaction mechanisms with reaction rates and selectivity as a function of catalyst composition. To study adsorbates on multiple supported catalyst samples, a flow reactor was designed and built (see Fig. 3). The reactor, made entirely of stainless steel ultrahigh vacuum components, allows the simultaneous IR transmission spectroscopic study of up to seven supported catalyst pellets. The number of pellets in this case was restricted mainly by the minimum diameter with which the individual pellets can be easily pressed and the maximum field of view that can be obtained with our specific optical setup. The FPA size does not restrict the number of samples, since theoretically, one array element per sample should be sufficient and, if necessary, larger arrays (over 250,000 pixels) can be obtained. Each catalyst sample is 6 mm in diameter and rests on a small ledge machined into each channel. The reactor is heated with three heating cartridges that

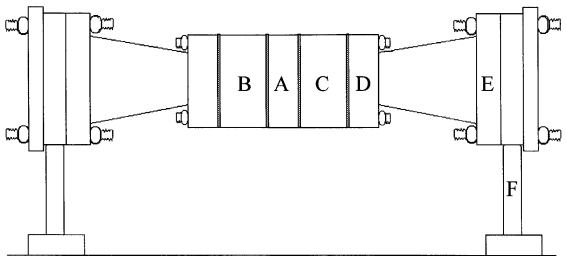

Fig. 3. Main parts of the flow reactor: (A) main flange containing samples, heating cartridges, and thermocouples; (B) gas inlet flange; (C) gas outlet flange with vacuum gauge; (D) conical flange; (E) outer flange containing IR-transparent windows; (F) standard optical table mounts.

slide into symmetrically spaced holes in the edge of the flange. The temperature is monitored with thermocouples located in holes machined into the flange. The flanges mounted on either side of the center flange are connected to the gas inlet/outlet system. The gas inlet system is equipped with three mass flow controllers, the outlet is pumped with a mechanical pump that can maintain pressures below 10 mTorr, and the total pressure in the reactor is monitored with a pressure gauge attached directly to the outlet flange. It should be noted here that this reactor can be used at pressures from 1 atm down to high vacuum by employing the appropriate pumping system. The ends of the reactor are fitted with conical flanges that hold infrared transparent CaF_2 windows. Thermal stresses on the windows resulting from heating the reactor are minimized by cooling water forced through copper tubing wrapped around the conical part of the flanges. This system is well suited for parallel IR transmission studies of adsorbates on the catalyst pellets. In this configuration, all catalysts in the reactor are exposed to the same reactant stream, share a common outlet stream, and are subjected to identical pretreatments.

2.3. Sample preparation

The purpose of our preliminary studies presented here is to establish that FTIR imaging can be used to monitor adsorbates on supported catalysts and to follow reaction products in the gas phase. The model system we chose was CO adsorption on different catalysts and CO oxidation. The supported catalyst samples used in this study were the transition metals, Pt, Pd, Ni, Rh, and Ru supported on silica (SiO_2) and γ-alumina (γ-Al_2O_3), as well as Cu-ZSM5. The supported catalysts were all synthesized using incipient wetness. All catalysts were subsequently calcined in air at 573 K for 6 h, and reduced at 473 K in 20% H_2/He for 12 h. All catalysts were pretreated simultaneously in the reactor by flowing oxygen or hydrogen over the pellets in cycles; the reactor was typically kept at 473 K during H_2 pretreatment and at 573 K during O_2 pretreatment. The total gas pressure for both oxidation and reduction was 200 mTorr.

3. Results and discussion

3.1. Study of CO adsorption on Cu-ZSM5 and Pt/SiO_2

The first example shown here is the investigation of the adsorption of carbon monoxide on both Cu-ZSM5 zeolite samples and silica supported platinum (Pt/SiO_2) catalysts. Adsorption of CO was used as a model system to demonstrate the capability of our experimental setup to monitor adsorbate monolayers on supported catalyst pellets. The reactor holding seven supported catalyst pellets was used to examine the samples in situ in the transmission mode. Three Pt/SiO_2 and three Cu-ZSM5 pellets were loaded into the reactor. CO mainly adsorbs on Pt/SiO_2 in a linear configuration, which produces a characteristic absorption band between 2060 and 2090 cm^{-1}, depending on the specific pretreatment and the CO coverage [41–43]. CO adsorbed on Cu-ZSM5 creates several groups of absorption bands, all located above 2100 cm^{-1}, which have been assigned to CO in different adsorption states [44,45], however, the exact band assignment is still somewhat unclear.

In order to demonstrate the quality of the spectral data, Fig. 4 shows two representative spectra of CO adsorbed on Pt/SiO_2. Spectrum A was taken with our imaging spectrometer in rapid-scan mode using the signal from one pixel, corresponding to a $\sim 300 \times 300\,\mu m^2$ sample area. Spectrum B was acquired in transmission mode from a single catalyst pellet (10 mm diameter) mounted in a single-pellet reactor with a conventional, non-imaging FTIR spectrometer equipped with a liquid nitrogen cooled MCT

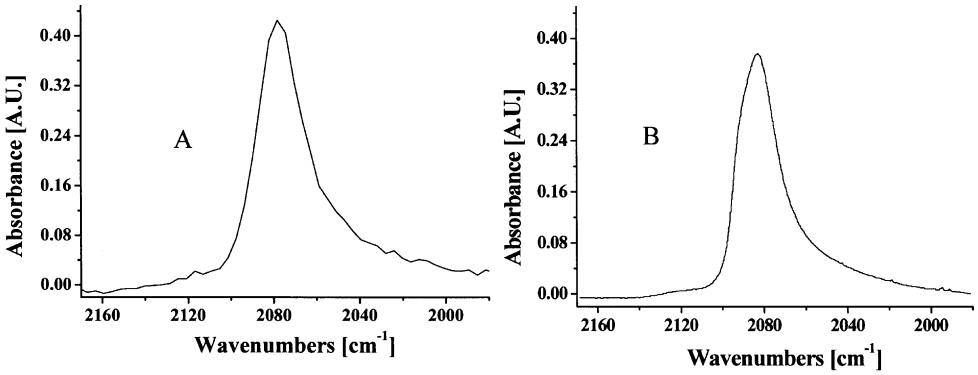

Fig. 4. Two representative FTIR spectra of CO adsorbed on a Pt/SiO_2 catalyst. The spectrum in (A) is from a single pixel ($\sim 300 \times 300\,\mu m^2$ area) of the imaging system described here and that in (B) is from a standard, non-imaging FTIR setup ($\sim 1\,cm^2$).

detector. Both spectra represent one scan, and no co-addition of spectra was performed. From this comparison, it becomes immediately clear that rapid-scan imaging is indeed capable of producing high quality data for similar collection parameters.

Due to the different frequencies of the CO absorption bands on the zeolite and the supported platinum catalyst, it becomes possible to distinguish between different adsorption states, and therefore different catalysts, in situ by creating spectral images at the appropriate frequencies. Fig. 5 shows a spectral image generated by plotting the absorbance values at $2080\,cm^{-1}$ for each pixel in the FPA. The three Pt/SiO_2 catalyst pellets can be unambiguously identified in the image (high absorbance intensity at $2080\,cm^{-1}$), while the other pellets do not show any intensity. Each point of this image also contains a full IR spectrum. Therefore, it becomes possible to study adsorption of gases on

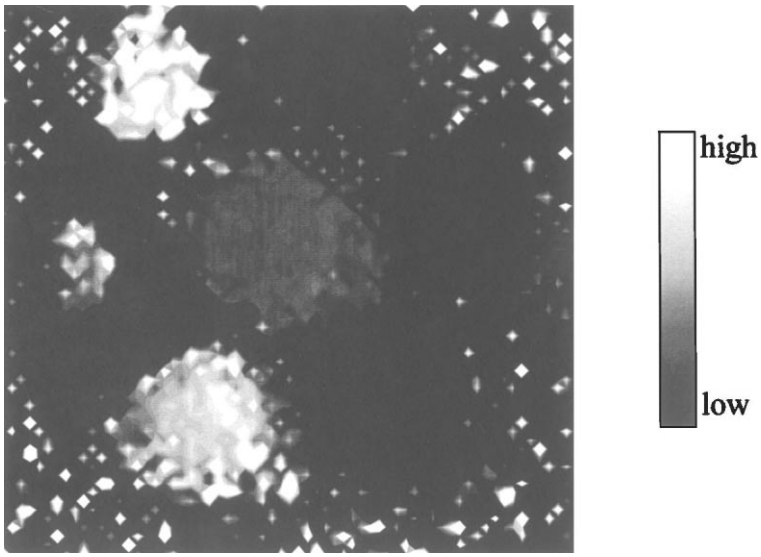

Fig. 5. Spectral image of the reactor showing the location of three Pt/SiO_2 pellets. The image was generated by plotting the absorbance intensity of the $2080\,cm^{-1}$ band (corresponding to CO adsorbed on Pt/SiO_2) for each pixel in the image. The diameter of each catalyst pellet is 6 mm.

multiple catalyst samples that have received identical pretreatment and are subject to the same gas stream, thereby avoiding any ambiguity with respect to pretreatment or dosing conditions.

3.2. Dynamics of CO adsorption on supported Pd, Pt and Rh

A library of supported transition metal catalysts was also studied for CO adsorption and CO oxidation. The reactor was loaded with two pellets of 3.5 wt.% Pt/SiO_2, two pellets of 1 wt.% $Pt/\gamma\text{-}Al_2O_3$, one pellet of 1 wt.% $Pd/\gamma\text{-}Al_2O_3$, and one pellet of 0.2 wt.% $Rh/\gamma\text{-}Al_2O_3$. One sample composed of SiO_2 support material was included as a control. To obtain background infrared spectra, four single beam reference spectra of the clean catalysts were acquired and co-added. CO was then introduced into the reactor at 200 mTorr, and single beam spectra (one scan) were collected every minute over a time span of 30 min with the CO pressure held constant. The spectra collected after dosing the CO were ratioed against the co-added background. Five representative spectra from the resulting collection of absorption spectra are shown for each catalyst type in Fig. 6. The spectra were smoothed with a 3-point adjacent averaging algorithm, and the CO peak areas (shown in Fig. 7) were calculated using numerical integration of the spectra after baseline correction.

.2% Pt/SiO_2: The spectra of CO adsorbed on Pt/SiO_2 shown in Fig. 6A demonstrate two adsorption bands that increase with CO exposure. The band above

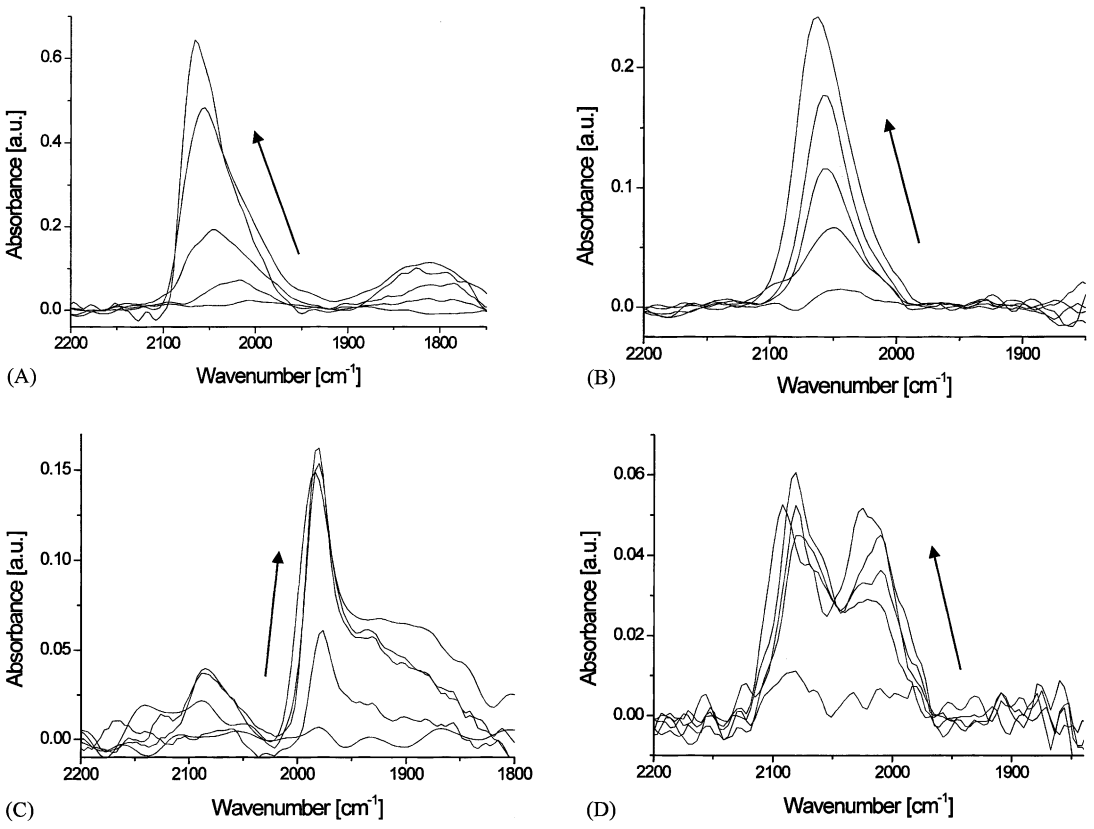

Fig. 6. Representative FTIR spectra from four different catalyst pellets acquired during CO dosing. The arrows indicate the direction of peak intensity change with dosing time. The catalysts are (A) 3.2 wt.% Pt on SiO_2, (B) 1 wt.% Pt on $\gamma\text{-}Al_2O_3$, (C) 1 wt.% Pd on $\gamma\text{-}Al_2O_3$, and (D) 0.2 wt.% Rh on $\gamma\text{-}Al_2O_3$.

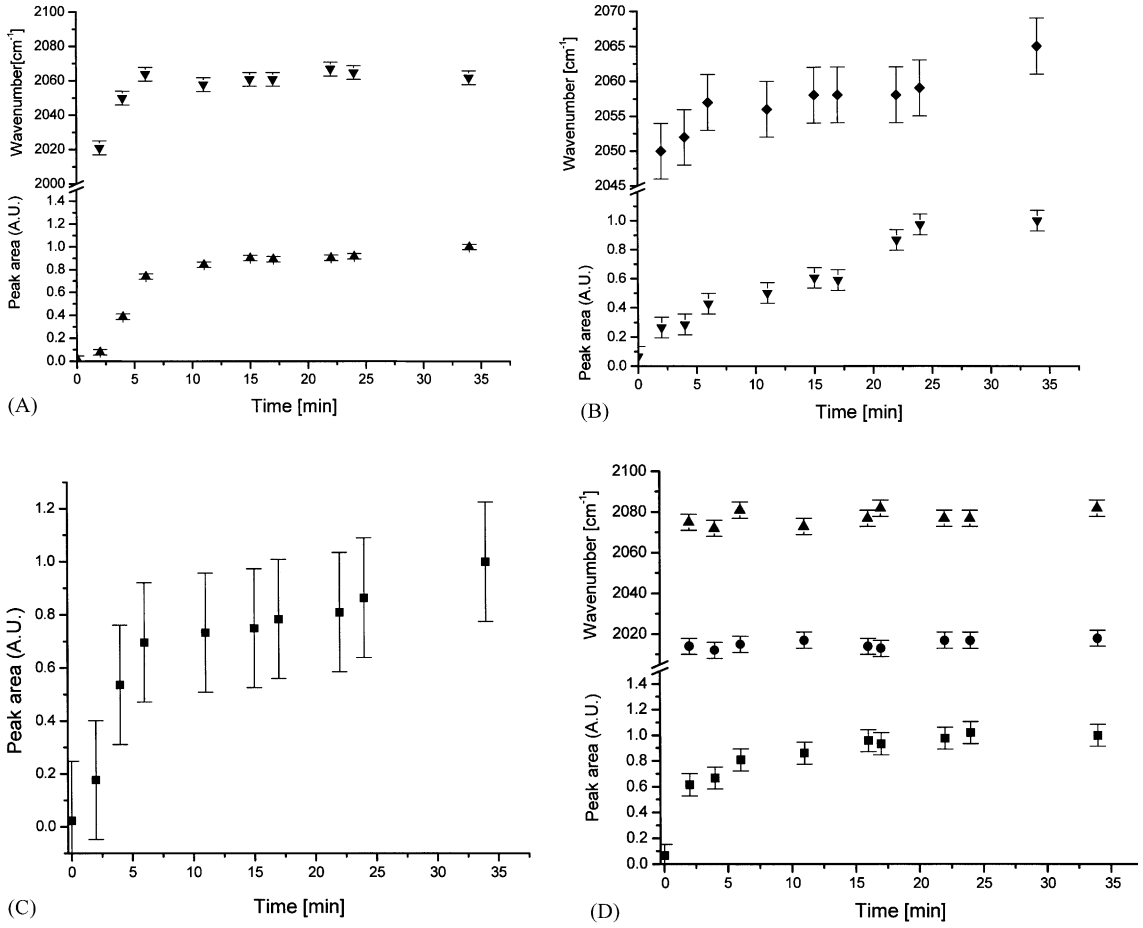

Fig. 7. Peak area and peak position as a function of total CO dosing time for same catalysts described in Fig. 6.

2000 cm^{-1} is assigned to linearly adsorbed CO [46]. The peak position of this band shifts with increasing coverage from 2020 to 2067 cm^{-1}, which can be explained by an increase in dipole coupling between the adsorbed CO molecules on the surface as the CO coverage increases [47]. The absorption band below 1900 cm^{-1} has a much lower intensity and is assigned to CO adsorbed on three fold sites [46]. Its position also shifts, albeit slightly less, with increasing coverage from 1807 to 1820 cm^{-1}. A plot of integrated peak area for the linearly bonded CO (Fig. 7A) shows that the peak area increases rapidly, then remains practically unchanged after 5 min approximately, indicating that all sites available for adsorption have been saturated. The peak position of this band also reaches its final value at the same time the peak area saturates.

1% Pt/γ-Al_2O_3: The CO absorption spectra for the Pt/γ-Al_2O_3 catalyst (Fig. 6B) show no peaks in the spectral region below 2000 cm^{-1}, indicating the absence of CO in higher coordinated adsorption sites. The only observed absorption band, assigned to linear-bonded CO, shifts from 2050 to 2066 cm^{-1} during dosing. The integrated peak area and peak position versus time (Fig. 7B) demonstrates a different pattern from the one observed for Pt/SiO_2. In the first 7 min, a peak shift of $\sim$17 cm^{-1} is observed with increasing coverage, followed by a steady increase in

the integrated peak area, although the peak position now remains almost unchanged.

1% Pd/γ-Al_2O_3: At least three CO adsorption bands are apparent in the spectra for Pd/Al_2O_3, shown in Fig. 6C. The small peak around 2084 cm^{-1} is assigned to linearly bonded CO [46]. At 1985 cm^{-1}, the most intense peak of the spectrum is observed. Its peak position shifts only slightly to higher wavenumbers as the coverage increases (from 1983 to 1989 cm^{-1}). This peak is assigned to bridge-bonded CO [46]. Around 1900 cm^{-1} is an additional broad peak, which is most likely a collection of multiple peaks from CO adsorbed on hollow sites. Linearly bonded CO on Pd/Al_2O_3 is reported at 2080 cm^{-1}, and bridge-bonded CO is reported at 1936 cm^{-1} [48]. The plot of integrated peak area of all peaks as a function of time (Fig. 7C) demonstrates similar behavior to the above examples, with equilibrium being reached after roughly 7 min. However, in this case, it is more difficult to evaluate the exact peak position for the bridge-bonded CO band since it overlaps with the broad peak around 1913 cm^{-1}.

Rh/γ-Al_2O_3: The spectra of CO adsorbed on Rh/γ-Al_2O_3 (Fig. 6D) demonstrate a doublet that can be assigned to two CO molecules chemisorbed onto a single Rh atom. The $Rh(CO)_2$ exhibits the doublet around 2083 cm^{-1} (asymmetric stretch) and around 2021 cm^{-1} (symmetric stretch). The peak positions of the doublet peaks do not shift (within error) as the exposure increases. This lack of shift has been attributed to the site being an atomically dispersed site [46]. A peak for linearly adsorbed CO is not observed, which is in agreement with the findings of Cavanagh and Yates [49], who studied CO adsorption on Rh/γ-Al_2O_3 with the same loading level. The plot of integrated peak area vs. time (Fig. 7D) rapidly increases in the beginning, then remains roughly constant until full coverage is reached after 15 min. The low overall CO absorbance intensity can be attributed to the low metal loading of this catalyst, which is only 0.2 wt.%.

In summary, these two feasibility experiments have clearly demonstrated that our instrumental setup is capable of studying the adsorption of gases onto multiple supported catalyst samples in a single experiment. An entire set of adsorption experiments for up to seven catalysts can now be performed in less than 1 day, including identical pretreatment for all catalysts in the reactor.

3.3. Applications of FTIR imaging to high-throughput screening — parallel reaction product analysis via gas-phase imaging spectroscopy

The main focus of parallel high-throughput analysis of heterogeneous catalysts is to rapidly analyze reaction products from individual library elements. This information, together with information about the presence of different adsorbates on the catalysts, allows us to systematically correlate reaction mechanism and catalyst performance with material properties in a catalyst library. Although several novel experimental approaches have been developed in the past few years, truly parallel product analysis has been one of the key bottlenecks in the application of high-throughput screening to heterogeneous catalysis.

For this purpose, a novel gas-phase sampling accessory has been developed in our laboratory. FTIR spectroscopy is a well-established tool for the analysis of the composition of gas mixtures [40]. Typically, 1–10 cm path length cells are used for routine gas analysis, while for trace gas analysis, longer path lengths are often necessary. The lower detection limit depends on several factors, such as the absorptivity of the absorption bands, the spectral noise level, and the strength and structure of the bands of interfering gases. Our novel technique allows us to examine the product streams of many reactors simultaneously with both FTIR and mass spectrometry.

The new reactor we have designed has individual channels holding one sample each with individual gas outlets, each of which is connected to small gas sampling cells. These cells are made of a stainless steel body with IR transparent windows sealed by O-rings and are arranged in an array fashion, so that many cells can be studied simultaneously using the FTIR imaging system. This allows us to obtain gas-phase spectra of the product streams in a parallel fashion. After the gas sampling cells, the gas outlets are directed to an array of valves, which leads to the inlet of a differentially pumped mass spectrometer.

In order to demonstrate the applicability of gas-phase IR imaging to reaction product analysis, we present here the preliminary results obtained from our reactor/gas-phase array setup, in which a simultaneous FTIR/MS analysis was used to determine light-off temperatures and conversion during CO oxidation over a commercial catalyst monolith. For calibration

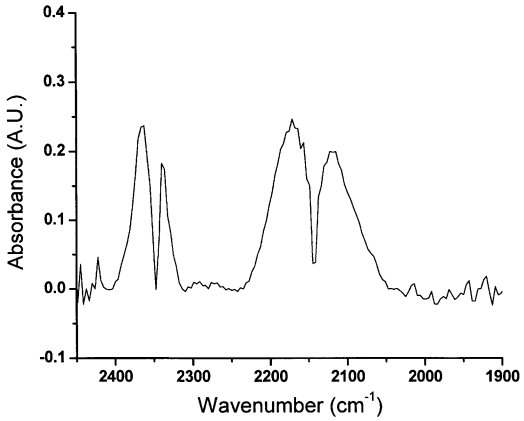

Fig. 8. Representative gas-phase spectrum of CO and CO_2 acquired with an FTIR imaging spectrometer equipped with a gas-phase sampling cell. The characteristic doublets of CO centered around 2143 cm^{-1} and CO_2 centered around 2350 cm^{-1} can be clearly observed.

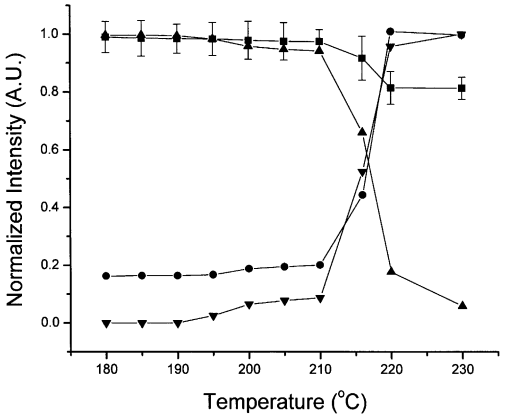

Fig. 9. Results of a light-off temperature study for CO oxidation on a commercial catalyst using a simultaneous FTIR/MS approach. The CO_2 concentration was measured simultaneously by FTIR (▼) and MS (●). The CO concentration was measured using FTIR (▲) and the O_2 concentration was determined by MS (■). The error bars shown are representative for all data.

purposes and to follow gases with no IR absorption, a differentially pumped mass spectrometer is attached to the outlet of the system. Fig. 8 shows a typical spectrum of gas-phase carbon monoxide taken from a single pixel of an image of a gas-phase cell using our imaging spectrometer setup. As an example for the feasibility of following reaction products with this combined MS/gas-phase FTIR spectrometer arrangement.

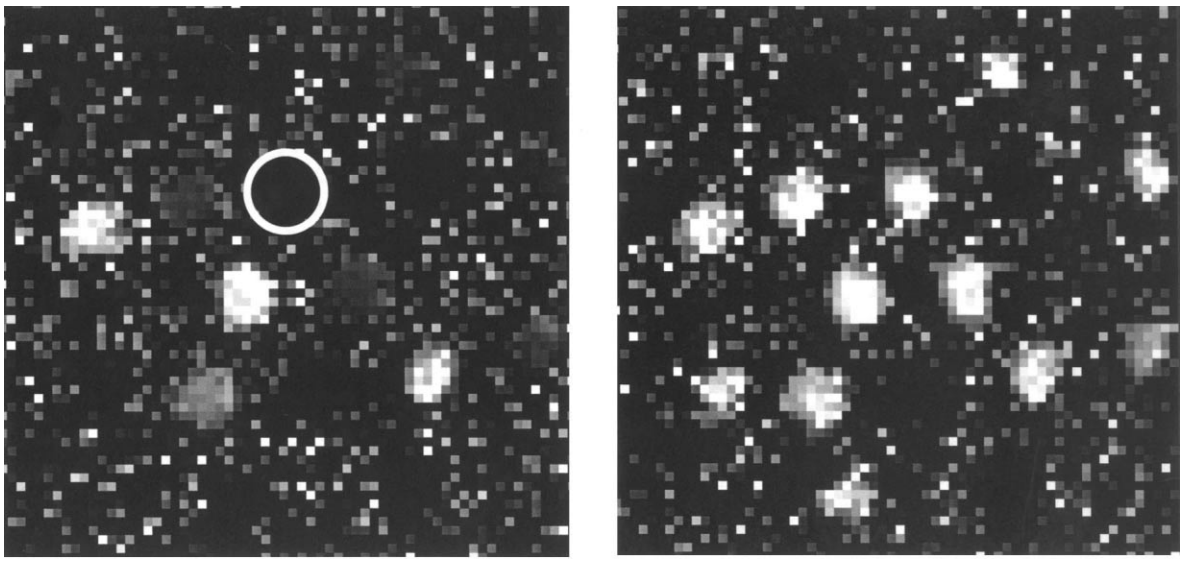

Fig. 10. Spectral images of CO_2 concentration (2360 cm^{-1}) measured by FTIR imaging. (A) at 430 K and (B) at 480 K. Light-off between these two temperatures can be seen for several elements, one of which is highlighted by a white circle in (A).

The data for CO_2 were taken both with the mass spectrometer and FTIR spectrometer and show very good agreement. The data for CO and oxygen show that with increasing reaction rate, both concentrations decrease. In this case, only CO was measured with IR spectroscopy, since oxygen is IR inactive and was therefore followed by mass spectroscopy. With this approach, it now becomes possible to follow reactants and products in the exit stream in a quantitative manner and to therefore determine conversions and selectivities.

Using the multi-sample array, not only does this technique allow rapid parallel identification of active catalysts, but also allows us to quantify reactivity and selectivity. Here we present preliminary data from a 16-element gas-phase array, which is coupled to a reactor system capable of holding 16 catalysts in powder form. The reaction performed was CO oxidation, and the reactor setup was loaded with different supported catalysts (Pt, Pd, and Rh on Al_2O_3 or SiO_2) and blank support materials. After 0.2 g of each catalyst sample was loaded, the reactor was closed and parallel pretreatment was performed via several oxidation and reduction cycles. The catalysts were cooled to room temperature under flowing nitrogen, and a reaction mixture of 10% CO in oxygen was added. A temperature ramp of 10 K/min was established, and absorbance images of the exit stream of all 16 samples were taken at every 30 s over 30 min, spanning a temperature range from 300 to 600 K. Fig. 10 shows representative absorbance images for the gas-phase CO_2 vibration band for reactor temperatures of 430 and 480 K. High intensity in the image indicates an active catalyst producing CO_2, and immediately it becomes clear that between these two temperatures, two catalyst samples have started to produce CO_2. In total, it took 30 min to assess the light-off characteristics and reactivity of the entire catalyst array over the range of 300 K. With the temporal resolution of our analytical technique, it becomes possible to change control parameters of the reaction (i.e., temperature, gas composition) on a timescale of seconds.

4. Conclusions

In summary, FTIR spectral imaging is capable of the simultaneous measurement of IR spectra of multiple members of a catalyst library, allowing in situ, parallel investigation of chemical processes such as adsorption, diffusion, and reaction. The experimental results presented in this paper demonstrate that rapid-scan FTIR imaging is ideally suited to study both adsorbates on members of supported catalyst libraries and gas-phase reaction products from these libraries in a truly parallel fashion. In all the experiments, the supported catalysts undergo the same pretreatment and identical dosing and reaction conditions. This not only saves time but also provides a more realistic basis for comparison between the different catalyst samples. Using rapid-scan FTIR imaging, it typically takes less than 20 s to acquire one full spectral data set, which permits not only rapid screening of reactivity, but also time resolved studies of phenomena like adsorption onto supported catalysts.

Acknowledgements

The authors would like to thank the National Science Foundation for financial support under grants CTS-9871020 and CTS-0071020.

References

[1] A.W. Czarnik, S.H. DeWitt, A Practical Guide to Combinatorial Chemistry, American Chemical Society, Washington, DC, 1997.
[2] X. Williard, I. Pop, L. Bourel, D. Horvath, R. Baudelle, P. Melnyk, B. Deprez, A. Tartar, Eur. J. Med. Chem. 31 (1996) 87.
[3] W.A. Warr, J. Chem. Info. Comp. Sci. 37 (1997) 134.
[4] W.H. Weinberg, E.W. McFarland, Tibtech 17 (1999) 107.
[5] X.-D. Sun, K.-A. Wang, Y. Yoo, W.G. Wallace-Freedman, C. Gao, X.-D. Xiang, P.G. Schultz, Adv. Mater. 9 (1997) 1046.
[6] S. Senkan, K. Krantz, S. Ozturk, V. Zengin, I. Onal, Angew. Chem. Int. Edit. 38 (1999) 2794.
[7] S.M. Senkan, Nature 394 (1998) 350.
[8] S.M. Senkan, S. Ozturk, Angew. Chem. Int. Edit. 38 (1999) 791.
[9] W.F. Maier, G. Kirsten, M. Orschel, P.A. Weiss, Chim. Oggi. 18 (2000) 15.
[10] M. Orschel, J. Klein, H.W. Schmidt, W.F. Maier, Angew. Chem. Int. Edit. 38 (1999) 2791.
[11] C.E. Kibbey, in: A.W. Czarnik, S.H. DeWitt (Eds.), A Practical Guide to Combinatorial Chemistry, American Chemical Society, Washington, DC, 1997, p. 199.
[12] M.J. Shapiro, J. Chin, R.E. Marti, M.A. Jarosinski, Tetrahedron Lett. 38 (1997) 1333.

[13] M.J. Shapiro, M. Lin, B. Yan, in: A.W. Czarnik, S.H. DeWitt (Eds.), A Practical Guide to Combinatorial Chemistry, American Chemical Society, Washington, D.C, 1997, p. 123.
[14] P. Cong, R. Doolen, Q. Fan, D.M. Giaquinta, S. Guan, E.W. McFarland, D.M. Poojary, K. Self, H.W. Turner, W.H. Weinberg, Angew. Chem. Int. Edit. 38 (1999) 484.
[15] P. Cong, A. Dehestani, R. Doolen, D.M. Giaquinta, S. Guan, V. Markov, D. Poojary, K. Self, H.W. Turner, W.H. Weinberg, Proc. Natl. Acad. Sci. 96 (1999) 11077.
[16] J.M. Newsam, F. Schuth, Biotechnol. Bioeng. 61 (1999) 203.
[17] C. Hoffmann, A. Wolf, F. Schuth, Angew. Chem. Int. Edit. 38 (1999) 2800.
[18] B. Jandeleit, D.J. Schaefer, T.S. Powers, H.W. Turner, W.H. Weinberg, Angew. Chem. Int. Edit. 38 (1999) 2494.
[19] S.M. Senkan, S. Ozturk, Angew. Chem. Int. Edit. 38 (1999) 791.
[20] W.F. Maier, A. Holzwarth, H.W. Schmidt, Angew. Chem. Int. Edit. 37 (1998) 2644.
[21] R.C. Gore, Science 110 (1949) 710.
[22] V.J. Coates, A. Offner, E.H. Siegler, J. Opt. Soc. Am. 43 (1953) 984.
[23] W.J. Haap, T.B. Walk, G. Jung, Angew. Chem. Int. Edit. 37 (1998) 3311.
[24] P.J. Treado, I.W. Levin, E.N. Lewis, Appl. Spectrosc. 48 (1994) 607.
[25] E.N. Lewis, P.J. Treado, R.C. Reeder, G.M. Story, A.E. Dowrey, C. Marcott, I.W. Levin, Anal. Chem. 67 (1995) 3377.
[26] E.N. Lewis, A.M. Gorbach, C. Marcott, I.W. Levin, Appl. Spectrosc. 50 (1996) 263.
[27] L.H. Kidder, V.F. Klasinsky, J.L. Luke, I.W. Levin, E.N. Lewis, Nat. Med. 3 (1997) 235.
[28] E.N. Lewis, I.W. Levin, Appl. Spectrosc. 49 (1995) 672.
[29] C. Marcott, R.C. Reeder, E.P. Paschalis, D.N. Tatakis, A.L. Boskey, R. Mendelsohn, Cell. Mol. Biol. 44 (1998) 109.
[30] R. Mendelson, E.P. Paschalis, P.J. Sherman, A.L. Boskey, Appl. Spectrosc. 54 (2000) 1183.
[31] C. Marcott, R.C. Reeder, J.A. Sweat, D.D. Panzer, D.L. Wetzel, Vib. Spectrosc. 19 (1999) 123.
[32] S.J. Oh, J.L. Koenig, Anal. Chem. 70 (1998) 1768.
[33] C.M. Snively, J.L. Koenig, Macromol. 31 (1998) 3753.
[34] C.M. Snively, J.L. Koenig, J. Polym. Sci. 1999, 2353.
[35] R. Bhargava, T. Ribar, J.L. Koenig, Appl. Spectrosc. 53 (1999) 1313.
[36] C.M. Snively, J.L. Koenig, J. Polym. Sci. (1999) 2261.
[37] R. Bhargava, S.Q. Wang, J.L. Koenig, Macromolecules 32 (1999) 8982.
[38] C.M. Snively, S. Katzenberger, G. Oskarsdottir, J. Lauterbach, Opt. Lett. 24 (1999) 1841.
[39] C.M. Snively, J.L. Koenig, Appl. Spectrosc. 53 (1999) 170.
[40] P.R. Griffiths, J.A. de Haseth, Fourier Transform Infrared Spectrometry, Wiley, New York, 1986.
[41] R.K. Brandt, R.S. Sorbello, R.G. Greenler, Surf. Sci. 271 (1992) 605.
[42] R.K. Brandt, M.R. Hughes, L.P. Bourget, K. Truszkowska, R.G. Greenler, Surf. Sci. 286 (1993) 15.
[43] G. Bonilla, T.D. Pletcher, G. Haas, J. Lauterbach, React. Kinet. Catal. Lett. 65 (1998) 3.
[44] A. Zecchina, S. Bordiga, G. Spoto, D. Scarano, G. Petrini, G. Leofanti, M. Padovan, C.O. Arean, J. Chem. Soc. Faraday Trans. 88 (1992) 2959.
[45] C. Crisafulli, S. Scire, S. Minico, R. Maggiore, S. Galvagno, Appl. Surf. Sci. 99 (1996) 401.
[46] J.C. Campuzano, in: D.A. Kind, D.P. Woodruff (Eds.), The Chemical Physics Of Solid Surfaces and Heterogeneous Catalysis, Vol. 3, Elsevier, Amsterdam, 1990, p. 389.
[47] J. Lauterbach, G. Bonilla, T.D. Pletcher, Chem. Eng. Sci. 54 (1999) 4501.
[48] K. Almusaiteer, S.S.C. Chuang, J. Catal. 184 (1999) 189.
[49] R.R. Cavanagh, J.T. Yates Jr., J. Chem. Phys. 74 (1981) 4150.